Relativistic approach to photon-nucleon scattering

H. T. Williams
Department of Physics, Washington and Lee University, Lexington, Virginia 24450
(Received 19 May 1986)

A relativistic calculation of photon-nucleon elastic scattering in the energy range from 0 to 450 MeV in the laboratory is presented. It includes explicit contributions from s- and u-channel nucleon intermediate states, t-channel neutral pion states, and s-channel delta resonance states. Other processes are implicitly included via energy-dependent parameters in the resonance process. Comparison with experiments show an improvement over similar nonrelativistic approaches.

INTRODUCTION

The elastic scattering of a photon from a nucleon appears to be a very clean elementary process: The photon interacts electromagnetically and thus the interaction vertices should be well known. The nucleon is the simplest baryon and thus an understanding of its elementary processes should be a lowest order check of quark models of hadrons. The nucleon is also the simplest nucleus, and if one is to use photons to study properties of complex nuclei, it is first necessary to understand the elementary nucleon process. At the present time, elastic photon scattering is becoming a tool in nuclear physics, and experimental and theoretical work is progressing, while the elementary nucleon process remains poorly understood due both to inadequate experimental data and inadequate theoretical explanation. Information derived from photon scattering can be quite different from that of electron scattering, due to the presence of the second electromagnetic vertex at the target. For a composite target (considering quarks within the nucleon, or the nucleon as a constituent of nuclei), the single photon vertex in the target, typical of lowest order calculations of electron scattering, causes a cancellation of some of the contributions of positive and negative currents within the target. Such cancellations can be a calculational advantage, but also limit the amount of information obtainable from the process. Photon scattering, on the other hand, admits the possibility of both the incoming and outgoing photons attaching to the same target constituent, giving a contribution proportional to charge squared, and thus giving contributions which are additive, regardless of sign of the charge.

Photon scattering from nuclei is presently being pursued since it contributes supplementary (and sometimes new) information to results from established techniques in electron scattering. It is a technique for studying pion exchange currents, whose effects largely cancel in electron scattering—the Siegert theorem.[1] Photon scattering data, when combined with pion scattering and pion photoproduction data, can provide consistency checks and help in analysis and understanding of the pion-nucleus process. In the intermediate energy region, many nuclear processes are dominated by the 3-3 nucleon resonance, and the modification of the resonance propagator in the nuclear medium is a subject of current attention. Photon scattering in the resonance region allows resonances to be excited and deexcited via an on-mass-shell electromagnetic particle and thus allows a clear look at the medium modification effects. To extract these and other kinds of information from nuclear experiments, one must be able to reliably calculate the elementary photon-nucleon contributions, and this paper is intended to contribute towards this goal.

Photon scattering from the nucleon should allow a test of quark models of hadrons. Whether it is useful to consider the nucleus as simple a multiquark state, or as a multinucleon state admitting some quark effects, a study of the electromagnetic processes of a three-quark system should contribute to the understanding of how the quark many-body problem can be approached. Most attempts at a quark explanation of photon scattering have been focused on the energy region below pion threshold and extraction of the electric and magnetic polarizabilities.[2] While this paper will not examine the nucleus as a collection of quarks, to whatever degree it is successful in producing a simple model of photon scattering using relativistic graphical techniques, it will provide a theoretical framework for attempted quark explanations.

Two difficulties have retarded experimental investigation into elastic photon scattering. Only recently have techniques existed for the production of a high flux of monochromatic photons. Photon tagging facilities now exist in several laboratories (Bonn, Mainz, Illinois, MIT). New continuous beam electron machines are being designed with monochromatic photon capabilities (CEBAF, for example). On the output end of such experiments, radiative processes, and at higher energies the competing neutral pion production process, make discrimination difficult. Detector technology has progressed to the point where these discriminations are now reliably being made, and clean data are forthcoming. Older data on photon nucleon elastic scattering are being repeated and error bars are being reduced. Due to continuing experimental problems, the data, while covering the energy range of interest for applications to nuclear problems, are limited in angles. Forward scattering cross sections are available only by extraction from total photon cross sections using dispersion relations, and reliable scattering data exist primarily only in the range $60° <$ c.m. angle $< 130°$. Because of the large error bars on the extracted 0°

data, and the absence of good data in the forward and backward directions, there are not stringent experimental limits on the allowed angular distributions. Good data are required at forward and backward angles in the energy region of the 3-3 resonance to allow theoretical extraction of information about the resonance; its $E2$ coupling constant, and the degree of interference with competing processes.

Despite the apparent simplicity of the photon nucleon process, attempts to explain it theoretically have traditionally met difficulties. Some of these problems can be laid to uncertainty in the experimental results available for comparison, but theoretical inconsistencies exist which are not data dependent. Yet other inconsistencies await more and better data. Dispersion theoretic explanations of the process have run into a difficulty at the energy of the 3-3 resonance which has yet to be resolved. Experimental data at 90° at the resonance energy are consistently below predictions of dispersion theory, even when the real part of the theoretical cross section is set to zero.[3] While the discrepancy has been reduced, the best experimental data remain at least one standard deviation *below* the lower limit prescribed by unitarity.[4] Nonrelativistic approaches to understanding of the process have been undertaken to provide a model useful in the treatment of photon-nucleus scattering, but also with limited success. The most recent and most complete such approach uses photoproduction data to restrict allowed energy dependence of the photon scattering amplitudes (via Watson's theorem), and uses extrapolation of the photoproduction process to continue the scattering amplitudes off shell.[5] Despite fitting parameters and choices made in energy dependencies to produce best agreement with existing data, fits are poor at some angles and energies, and nuclear processes calculated using this model are thus limited in their accuracy and predictive ability. Relativistic approaches to understanding the scattering process have been hampered by a long existing misunderstanding concerning the propagator for the 3-3 resonance.[6,7]

THE CALCULATION

The differential cross section for the scattering of photons and nucleons will be calculated relativistically, in an attempt to match existing data from threshold to 450 MeV excitation. This should allow for the use of the results in nuclear calculations which encompass the 3-3 resonance region. The technique would allow simple extension to include higher mass nucleon resonances. In particular, the next heavier resonance, $N^*(1470)$, has the same spin and isospin as the nucleon and becomes a straightforward inclusion based on the nucleon calculations: Its influence upon the cross section may become important immediately above the 3-3 resonance peak.

Figure 1 shows the Feynman diagrams to be included in the calculations. All will be treated relativistically, thus including particle as well as antiparticle intermediate states. Conventions for four-vectors and for gamma matrices will follow Bjorken and Drell.[8] Such a diagrammatic approach necessarily leads to difficulties with unitarity. Truncation of the Hilbert space to include only

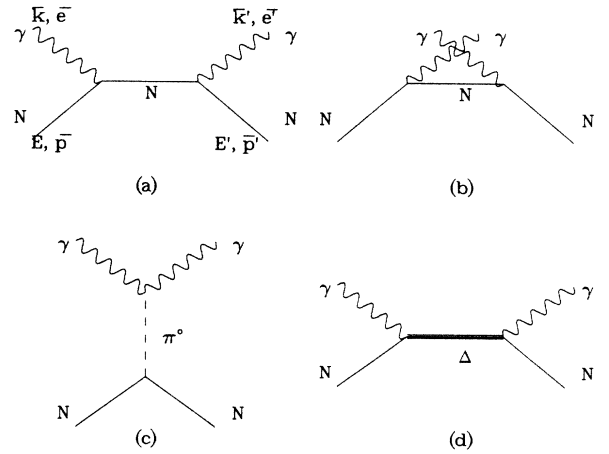

FIG. 1. Processes which contribute to elastic pion-nucleon scattering: (a) s-channel nucleon exchange; (b) u-channel nucleon exchange; (c) t-channel neutral pion exchange; (d) s-channel delta exchange. In (a) the variables in the center of mass system are labeled; momentum and polarization of the photons, energy and momentum of the nucleons.

selected processes leads to nonunitary amplitudes, and those aspects of unitarity which are important in the final results must be restored artificially.[9] This restoration in the present calculation will involve the use of an energy-dependent vertex function and resonance width for the 3-3 resonance.

Diagrams 1(a) and (b) represent the ordinary s- and u-channel nucleon graphs, and lead to the Klein-Nishina cross section when nucleon anomalous moments are ignored (these moments are of course included in the results of this work). The threshold value of the photon-nucleon scattering cross section, which must equal the Thompson cross section, is given exactly by the sum of these two contributions from nucleon intermediate states. The sum of the remaining contributions must necessarily vanish at threshold to give the proper value there. As energy increases, the actual cross section begins to deviate from the results of these two graphs due, at lower energies, to nucleon polarizability and finally to particle production thresholds.

Diagram 1(c) shows the exchange of a t-channel π^0, a process with vanishing contribution at threshold (consistent with the Thompson cross section being given by the nucleon graphs) but a non-negligible contribution in the energy region below and around the pion threshold. The fraction of the total cross section contributed by this process is largest at angles between 90° and 180° at about 150 MeV photon laboratory energy. Its contribution is particularly important in the extraction of nucleon polarizabilities, where the deviation of the cross section from the point nucleon behavior of diagrams 1(a) and (b) is the crucial experimental information. A contribution similar to 1(c), due to the t-channel exchange of an η^0, is easily included computationally, since the required algebra is the same as that for the π^0. It is not included here, since the mass of the η^0 (549 MeV) puts it more distant from the mass shell than the pion graph, and the coupling con-

stants for the eta are significantly lower than those for the pion.

Diagram 1(d) is the dominant contribution in the region above pion threshold to 500 MeV photon laboratory energy. It is obviously the source of the resonance behavior in the spin $\frac{3}{2}$ isospin $\frac{3}{2}$ channel, but due to the inclusion of negative energy states of the intermediate baryon, it also incorporates nonresonant background contributions in this and other angular momentum states. The companion u-channel delta excitation graph [similar to 1(b)] is not included in the present calculation. It, too, contributes nonresonant background to the cross section. At threshold, it yields a contribution equal to that of the s channel graph [of 1(d)]: Its relative importance decreases with increasing photon energy, and at the resonant energy, the u-channel delta is 600 MeV off mass shell, and has a small (and relatively uninteresting) contribution. The threshold contribution of the delta graphs does *not* vanish, and when combined with the nucleon intermediate states will produce a cross section in excess of the Thompson cross section and thus at variance with experiment at zero photon energy. This is a reflection of the problem of limiting the graphs to be included. Treating the complete Hilbert space of the scattering process, including all possible intermediate states in s, u, and t channels, would produce an amplitude which exhibits unitarity and, as well, satisfies the threshold requirement. A standard way of repairing this damage is to allow the $\gamma N\Delta$ vertex to show an energy dependence which vanishes at threshold. This energy dependence must be chosen to satisfy the threshold requirement, but unitarity can be utilized in the choosing of energy-dependent vertex functions and resonance widths which appropriately represent the omitted processes. Olsson[9] has carried out such a procedure in the case of pion photoproduction from the nucleon. He includes the expected pole terms, postulates a background term, and then lets the multichannel unitarity equations dictate the energy dependence of the width and vertices of the 3-3 resonance graph. In the case of photoproduction, the equation can be approximately solved due to the dominance of the πN over the γN final state. For photon scattering the equations remained coupled, and analytic results are difficult to achieve. Here, as a less satisfying alternative, unitarity is used as a justification for allowing energy dependences in the delta width and vertices. The Olsson procedure gives the proper threshold cross section, ensures the scattering amplitude to be real below pion threshold, and produces the correct resonance width and strength at resonance energy. The omission of the u channel delta process is thus justified in the energy region of interest: At threshold, where it is as important as the s-channel delta process, it is suppressed by a vertex factor which vanished at threshold; at higher energies it is small and slowly varying and is accounted for by the use of energy-dependent terms in the delta propagator.

The amplitudes for the processes illustrated in Figs. 1(a) and (b) make use of the N-N vertex and the nucleon propagator of Bjorken and Drell:[8]

$$(V_{\gamma NN})_\nu = -ie(\gamma_\nu + \sigma_{\nu\mu}k^\mu K/2m)\ ; \tag{1}$$

$$P_N(p) = i\frac{\not p + M}{p^2 - M^2}\ . \tag{2}$$

Letting k (k') represent the four-momentum of the incoming (outgoing) photon, and e (e') represent its polarization four-vector, p (p') the incoming (outgoing) four-momentum of the nucleon [Fig. 1(a)], and M and K the nucleon mass and anomalous moment, the invariant amplitudes for the s- and u-channel nucleon graphs are as follows:

$$T_{1a} = \bar u(p')[V^\dagger_{\gamma NN}\cdot e' P_N(p+k) V_{\gamma NN}\cdot e]u(p)\ ; \tag{3}$$

$$T_{1b} = \bar u(p')[V^\dagger_{\gamma NN}\cdot e P_N(p-k') V_{\gamma NN}\cdot e']u(p)\ . \tag{4}$$

The initial and final nucleon spinors are represented by $u(p)$ and $\bar u(p')$, respectively.

The amplitude for Fig. 1(c) requires the π^0NN vertex,[8] the $\pi^0\gamma\gamma$ vertex,[10] and the propagator for the π^0:[8]

$$V_{\pi NN} = g_0\gamma_5\tau_0\ ; \tag{5}$$

$$(V_{\pi\gamma\gamma})^{\alpha\beta} = g_1\epsilon^{\mu\nu\alpha\beta}k_\mu k'_\nu\ ; \tag{6}$$

$$P_\pi(q) = \frac{i}{q^2 - m^2}\ . \tag{7}$$

The pion mass is $m = 135.0$ MeV, and its coupling constants are $g_0 = 13.3$ (unitless), and $g_1 = 2.55\times 10^{-5}$ MeV as deduced from the lifetime of the π^0. The scattering amplitude contributed by t-channel neutral pion exchange is therefore

$$T_{1c} = \bar u(p')[V^\dagger_{\pi NN}\cdot e' V_{\pi\gamma\gamma}\cdot e P_\pi(p-p')]u(p)\ . \tag{8}$$

The resonant amplitude, represented in Fig. 1(d), requires for its calculation entities of lesser certainty. The Rarita-Schwinger formalism will be used to treat the spin $\frac{3}{2}$ particle within the Dirac spin $\frac{1}{2}$ algebra. There are two possible vertices which allow the coupling of a nucleon to a spin $\frac{3}{2}$ baryon via a photon: the $M1$ coupling,

$$V^{M1}_{\gamma N\Delta} = ig_{M1}\left[\frac{k e_\nu - \not e k_\nu}{M + M_\Delta}\right]\gamma_5\ ; \tag{9}$$

and the $E2$ coupling,

$$V^{E2}_{\gamma N\Delta} = -ig_{E2}\left[\frac{P_N\cdot e k_\nu - P_N\cdot k e_\nu}{(M+M_\Delta)^2}\right]\gamma_5\ . \tag{10}$$

Comparison of theory with photoproduction data shows the $E2$ coupling constant to be smaller than the $M1$ by a factor of 20;[11] in addition, the $E2$ vertex is smaller than the $M1$ due to an additional factor of (photon momentum/nucleon mass). In order to achieve the minimal set of amplitudes which should be expected to produce reasonable comparison with experiment, the $E2$ coupling is omitted from the calculations herein; this is consistent with quark model predictions of a vanishing $E2$ coupling, and experimental fits which argue to the smallness[12] of this contribution. The value of the $M1$ coupling constant used is $g_{M1} = 0.93$, consistent with the best value chosen to fit photoproduction data, and with quark model predictions. The propagator for spin $\frac{3}{2}$ particles in the Rarita-Schwinger formalism was derived by Behrends and Fronsdal,[13] but has suffered from frequent

misrepresentation in the intervening years.[7] The form used here is that of Behrends and Fronsdal.

$$P^{\mu\nu}=\frac{\not p+M_\Delta}{2M_\Delta(p^2-M_\Delta^2)}\left[g^{\mu\nu}-\tfrac{1}{3}\gamma^\mu\gamma^\nu-\frac{1}{3p^2}(\not p\gamma^\mu p^\nu+p^\mu\gamma^\nu\not p)\right]. \tag{11}$$

Gauge invariance and unitarity require that this form be supplemented by an energy dependence in the resonance width, as well as energy-dependent vertex functions. Without these additional energy dependencies, the Thompson limit is not satisfied at threshold, and the resonance contribution is complex, inappropriately, below pion threshold. These additional energy dependencies represent the implicit inclusion of other processes in the calculation. The u-channel delta graph (crossed photon lines), for example, should be as important as the resonant delta graph at photon threshold, and the vertex factors can be chosen to represent that contribution. Low energy theorems require the cross section to be that of pure charge scattering at photon threshold, and thus that the contributions other than intermediate s and u channel nucleon graphs must cancel. This cancellation requires dipole quark excitations [N*(1520), for example] as well as delta contributions.[2] Figure 2 shows how the cross section is altered by the inclusion of these energy dependencies. With a fixed width and no vertex function (curve a), the threshold cross section is several times too large, the resonance peak occurs at too high an energy, and the overall amplitude is too large. The peak could be shifted back by picking a delta mass less than 1232 MeV, but no *a priori* justification for this shift is seen. The amplitude could, of course, be adjusted downward by picking a smaller $\gamma N\Delta$ coupling constant, but this reduction moves the best fit coupling constant more distant from the values from quark models and photoproduction fits—this, too, is not desirable. Curve b in Fig. 2 shows the effect of an energy-dependent resonance width which vanishes at and below the pion-nucleon threshold. The particular energy dependence chosen is that of Olsson,[9]

$$\Gamma(q)=0.801\frac{q^3}{q^2+160^2}\ , \tag{12}$$

who deduced the form from the requirements of unitarity upon the nucleon and delta processes. The scattering amplitude contributed by s-channel delta exchange takes the form

$$T_{1d}=\bar u(p')(V_{\gamma N\Delta}^{M1+}\cdot P\cdot V_{\gamma N\Delta}^{M1})u(p)V(k^2,q^2)\ . \tag{13}$$

The results of Olsson regarding the vertex function are not as easily utilized, since he treated processes only above pion threshold (pion-nucleon scattering, pion photoproduction) where the photon-nucleon channel could be neglected when it was in competition with the pion-nucleon channel. No clue is given there for the behavior of the vertex factors below pion threshold. A phenomenological vertex function is used herein which has the proper behavior at the thresholds (proportional to k^2 at photon threshold, and to q^2 at pion threshold), is constant at high energies, and is algebraically simple:

$$V(k^2,q^2)=0.143\frac{k^2}{k^2+100^2}+1.03\frac{q^2}{q^2+70^2}\ . \tag{14}$$

The k^2 dependence is chosen to best represent the experimental cross section below $k=150$ MeV. While the zero photon energy cross section is given exactly by the nucleon intermediate states, the k^2 terms exhibit roughly equal contributions from nucleon, neutral pion, and baryon resonance intermediate states.[14] Since the s-channel delta amplitude dressed with these energy dependencies is to represent all higher contributions, it is valid to attempt to fit the low energy data using the vertex factor. The q^2 dependence must have proper threshold behavior and must force the vertex function to one at the resonance peak. The remaining freedom was used to reasonably approximate the shape of the experimental resonance curve. The cross section at 90° utilizing both Eqs. (12) and (13) is shown as curve c in Fig. 2.

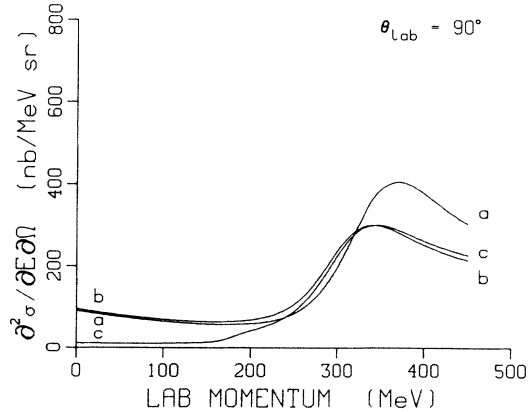

FIG. 2. The effect of an energy-dependent width and vertex factor on the differential cross section: (a) width =110 MeV, vertex factor =1; (b) energy-dependent width from Eq. (12), vertex factor =1; (c) energy-dependent width from Eq. (12), vertex factor from Eq. (13).

RESULTS

Figures 3–6 show the results of the present calculation compared to experimental data[15–20] at four angles. In the forward direction, experimental points are calculated from total photon cross sections using the optical theorem.[15] The angles 67° and 122° represent the most forward and most backward laboratory angles where a significant amount of photon scattering data exist. To preserve the simplicity of this approach, it was decided to choose a single resonance mass and $\gamma N\Delta$ coupling constant which would reasonably reproduce the existing data at all angles and at energies between threshold and 450 MeV photon laboratory energy. Changing the resonance mass would in no case improve the match to the data. A slightly lower coupling constant could improve the fit at 62°, but at the expense of the fits at other angles. All of the results shown (Figs. 2–9) are calculated using a resonance mass of 1232 MeV, and a coupling constant of $g_{M1}=0.93$. This value, chosen to fit the elastic scattering data, com-

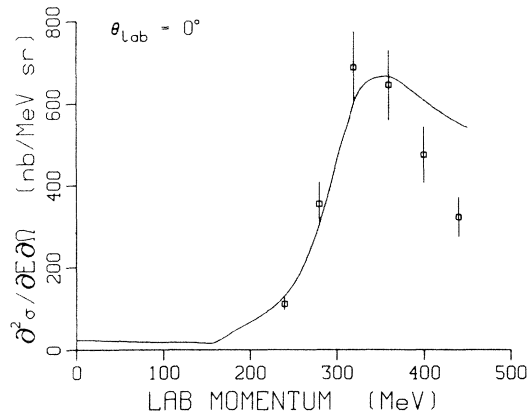

FIG. 3. Calculated differential cross section (solid line) at 0° shown with data extracted from total cross section data, Ref. 15.

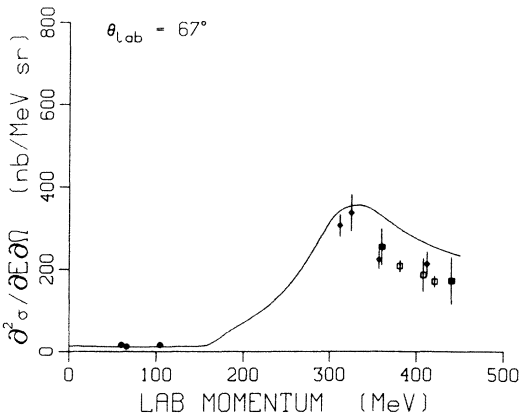

FIG. 4. Calculated differential cross section (solid line) at 67° shown with accumulated data in the range 60°—75°. Open boxes are data of Genzel, Ref. 15; diamonds are data of DeWire, Ref. 17; shaded boxes are data of Nagashima, Ref. 18; shaded circles are data reported in Baranov and Fil'kov, Ref. 20.

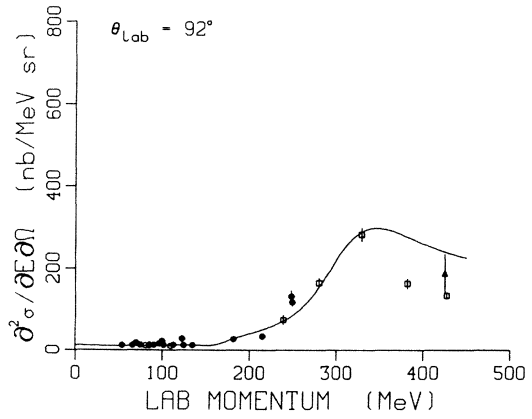

FIG. 5. Calculated differential cross section (solid line) at 92° shown with accumulated data in the range 85°—100°. Open boxes are data of Genzel, Ref. 15; open circles are data of Baranov, Ref. 19; triangles are data of Ishii, Ref. 16; shaded circles are data reported in Baranov and Fil'kov, Ref. 20.

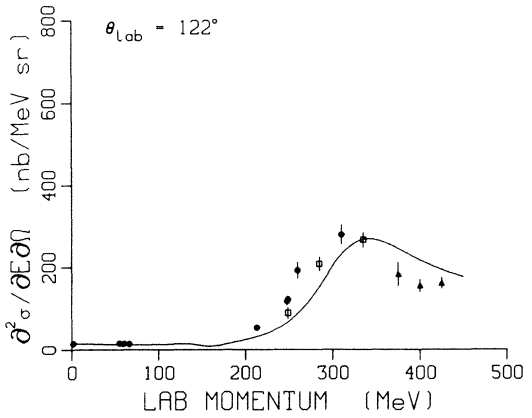

FIG. 6. Calculated differential cross section (solid line) at 122° shown with accumulated data in the range 115°—130°. Open boxes are data of Genzel, Ref. 15; triangles are data of Ishii, Ref. 16; shaded circles are data reported in Baranov and Fil'kov, Ref. 20.

pares with values from analyses of photoproduction data which range from 1.08 to 1.42, an SU(3) value of 1.15, and an SU(6) value of 0.92.[9,21,22] The nearness of the present value to that deduced from SU(6) is interesting, but most likely coincidental, given the approximate nature of most SU(6) predictions of elementary particle properties. For each of the four angles in Figs. 3—6, the present model accurately predicts the low energy behavior ($0 < k < 200$ MeV), as well as the position and height of the resonance peak. The best reproduction over the whole energy range is at 90°, but the experimental data there are not consistent, so the fit may not be as good as it might appear. The data in cases where two experiments are done at comparable energies and angles show discrepancies beyond the statistical error bars. Before conclusive results can be drawn from comparison of experiment and theory, consistent and accurate data over a large range of angles and energies are necessary. The most consistent problem with the present calculations is at energies above the resonance peak. The overestimate of the cross section, most severe at 0°, could be rectified by a more complicated energy dependence for the resonance width or vertex factors. Because of the angular dependence of the discrepancy, however, it seems likely that the high energy results can be well matched only with the explicit inclusion of higher resonances. The $N^*(1470)$ spin and isospin $\frac{1}{2}$ resonance will provide a growing contribution in the energy range beyond the delta peak, and its angular dependence will differ from that of the delta so as to give angular-dependent corrections. The low energy side of the delta peak also exhibits experiment-theory disagreement. These, too, could be better understood with more (and more consistent) data; could be diminished by use of a more complicated vertex factor; or could be the result of processes not considered. The results of Dreschel and Russo,[2] implying the importance of at least the 1520 MeV resonance in the threshold result, imply that this energy range could be greatly influenced by higher s-channel resonances.

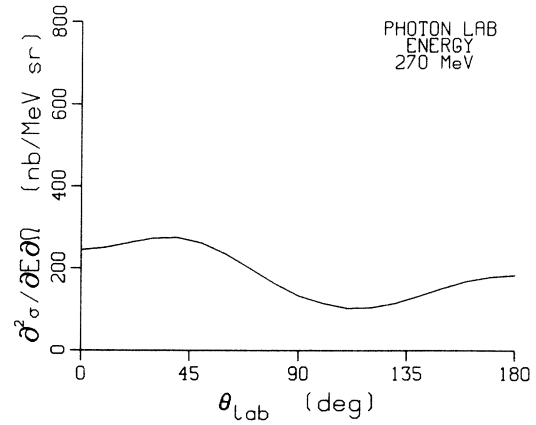

FIG. 7. Calculated differential cross section versus laboratory angle at laboratory momentum corresponding to resonance energy minus 55 MeV (in the center of mass).

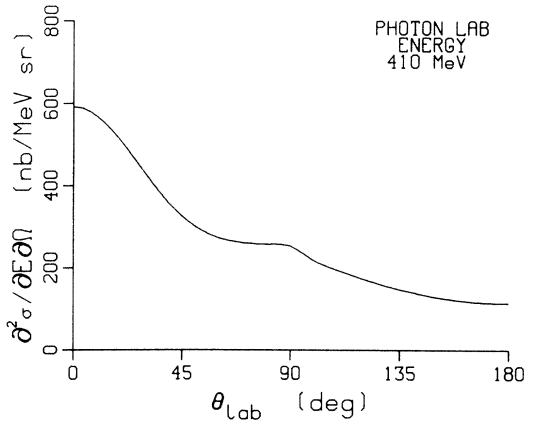

FIG. 9. Calculated differential cross section versus laboratory angle at laboratory momentum corresponding to resonance energy plus 55 MeV (in the center of mass).

It is significant that, while the calculation by no means produces a good fit to the data, it uses reasonable coupling constants and masses to give a good representation of the general shape and size of the cross section energy and angular dependencies. Koch, Moniz, and Ohtsuka,[5] using a nonrelativistic approach to the problem, find the need for considerable contribution from an s-wave "background" term, in addition to the resonant process which was calculated using $f_{\gamma N\Delta}=1.03$. This implies that the majority of the necessary background contribution can be found in the relativistic amplitude for the process of diagram 1(b). The part of this calculation which corresponds to an antibaryon in the intermediate state consists of terms of all multipolarities which are contributing in the resonance region. The magnitude and energy dependence of this background contribution are thus fixed by the resonance parameters.[7]

Figures 7–9 show the angular dependence of the laboratory cross section at the resonance energy and one half width above and below resonance energy. The variation from the relatively isotropic distribution below resonance to the striking forward asymmetry at resonance and above shows the importance of nonresonant contributions at and around the resonance energy. The $[7+3\cos^2(\theta)]$ angular distribution expected from the decay of a $p^{3/2}$ state is considerably altered by angular distributions from other multipoles associated with the relativistic expression of the delta excitation process [Fig. 1(d)]. Consistent data over a much wider range of angles than is presently available will be necessary before these predictions can be reliably evaluated.

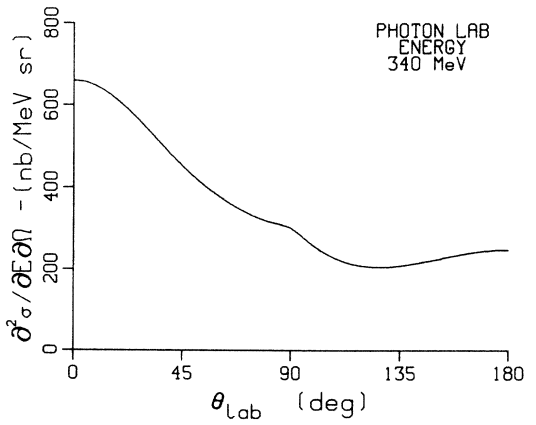

FIG. 8. Calculated differential cross section versus laboratory angle at laboratory momentum corresponding to resonance energy.

CONCLUSION

A simple tree graph approach to the calculation of pion-nucleon scattering up to 450 MeV has been presented. It has shown that considerable contribution from baryon resonances of higher mass than the delta (1232 MeV) as well as from u-channel resonance graphs is necessary to fit existing data without *ad hoc* form factors and energy dependence in the resonance width. It is shown however, that a big part of the background which is necessary to add in nonrelativistic calculations is accounted for by the use of relativistic wave functions and propagators. Data with smaller errors (systematic errors, in particular) over a wide range of angles will help indicate if the addition of a few more graphs will considerably improve the predictions, or whether it will be necessary to approach the problem in a significantly different way. The need to incorporate u-channel resonance graphs renders the calculation much more difficult, but more significantly it leads to the problem of defining propagators for baryons with spin $>\frac{1}{2}$ which are valid in many-body intermediate states. The success of work with quark models to determine nucleon polarizabilities leads to the hope that quark models might more simply describe the resonance region for this process. Relativity will doubtless be an important part of such a quark calculation.

The author would like to acknowledge the help of James Coyle and Karl Keller, who made considerable contributions to the numerical computations.

[1]J. F. Siegert, Phys. Rev. **52**, 787 (1937).
[2]D. Dreschel and A. Russo, Phys. Lett. **137B**, 294 (1984), and references therein.
[3]W. Pfeil, H. Rollnik, and S. Stankowski, Nucl. Phys. **B73**, 166 (1974).
[4]D. M. Akhmedov and L. V. Fil'kov, Yad. Fiz. **33**, 1083 (1981) [Sov. J. Nucl. Phys. **33**, 573 (1981)].
[5]J. H. Koch, E. J. Moniz, and N. Ohtsuka, Ann. Phys. (N.Y.) **154**, 99 (1984).
[6]H. T. Williams, Phys. Rev. C **29**, 2222 (1984).
[7]H. T. Williams, Phys. Rev. C **31**, 2297 (1985).
[8]J. D. Bjorken and S. D. Drell, *Relativistic Quantum Mechanics* (McGraw-Hill, New York, 1964).
[9]M. G. Olsson, Nucl. Phys. **B78**, 55 (1974).
[10]G. K. Greenhut, Phys. Rev. D **1**, 1341 (1970).
[11]D. Schiff and J. Tran Than Van, Nuovo Cimento **48**, 1273 (1967).
[12]D. Schiff and J. Tran Than Van, Nuovo Cimento **48A**, 1273 (1967).
[13]R. E. Behrends and C. Fronsdal, Phys. Rev. **106**, 345 (1957).
[14]V. A. Petrun'kin, Fiz. Elem. Chastits At. Yadra **12**, 692 (1981) [Sov. J. Part. Nucl. **12**, 278 (1981)].
[15]H. Genzel, M. Jung, R. Wedemeyer, and H. J. Weyer, Z. Phys. A **279**, 399 (1976).
[16]T. Ishii *et al.*, Nucl. Phys. **B165**, 189 (1980).
[17]J. W. DeWire *et al.*, Phys. Rev. **124**, 909 (1961).
[18]Y. Nagashima, Ph.D. thesis, Institute for Nuclear Study, University of Tokyo Report TH-47, 1961, reported in P. S. Baranov and Fil'kov, Fiz. Elem. Chastits At. Yadra **7**, 108 (1976) [Sov. J. Part. Nucl. **7**, 42 (1976)].
[19]P. S. Baranov *et al.*, Yad. Fiz. **21**, 6 (1975) [Sov. J. Nucl. Phys. **21**, 355 (1975)].
[20]P. S. Baranov and L. V. Fil'kov, Fiz. Elem. Chastits At. Yadra **7**, 108 (1976) [Sov. J. Part. Nucl. **7**, 42 (1976)].
[21]A. J. Dufner and Y. S. Tsai, Phys. Rev. **168**, 1801 (1968).
[22]The vertex formula of Eq. (10) includes isospin dependence implicitly in the coupling constant, so it is not to be multiplied by isospin coupling coefficients. To compare with standard vertex notation of Refs. 9 and 21, the coupling constant of this paper should be divided by the coefficient $\sqrt{2}/3$.